University of Baghdad
College of Engineering
JOURNAL OF ENGINEERING

Journal of Engineering

journal homepage: www.joe.uobaghdad.edu.iq
Number 1 Volume 25 January 2019

Mechanical and Energy Engineering

Investigation of R134a Flow Boiling Heat Transfer and Pressure Drop in the Evaporator Test Section of Refrigeration System

Ahmed J. Hamad*
Engineering Technical College-Baghdad
Middle Technical University
Baghdad, Iraq
E-mail: ahmed.elhamad@yahoo.com

Zahraa Kareem Yasser
Engineering Technical College-Baghdad
Middle Technical University
Baghdad, Iraq
E-mail: zahraakareemk30@gmail.com

ABSTRACT

This paper presents an experimental and theoretical analysis to investigate the two-phase flow boiling heat transfer coefficient and pressure drop of the refrigerant R-134a in the evaporator test section of the refrigeration system under different operating conditions. The test conditions considered are, for heat flux (13.7-36.6) kW/m^2, mass flux (52-105) kg/m^2.s, vapor quality (0.2-1) and saturation temperature (-15 to -3.7) ˚C. Experiments were carried out using a test rig for a 310W capacity refrigeration system, which is designed and constructed in the current work. Investigating of the experimental results has revealed that, the enhancement in local heat transfer coefficient for relatively higher heat flux 36.6 kW/m^2 was about 38% compared to 13.7 kW/m^2 at constant operating conditions. The enhancement in heat transfer coefficient was about 57% when the mass flux increased from 52 kg/m^2.s to 105 kg/m^2.s at constant test conditions. The enhancement in the heat transfer coefficient was about 64% when the saturation temperature increased from -8 to -3.7 at fixed refrigerant mass velocity and heat flux. The effect of mass velocity on pressure drop was relatively higher by about 27% than that for heat flux at specified test conditions. The comparison between the experimental and theoretical results has shown an acceptable agreement with an average deviation of 21%.

Key Words: heat transfer, pressure drop, flow boiling, heat flux.

استقصاء انتقال الحرارة وانحدار الضغط لغليان مائع التثليج R134a في حالة الجريان في مقطع فحص لمبخر منظومة تجميد

أحمد جاسم حمد*
الكلية التقنية الهندسية – بغداد - الجامعه التقنيه الوسطى
العراق – بغداد

زهراء كريم ياسر
الكلية التقنية الهندسية – بغداد - الجامعه التقنيه الوسطى
العراق - بغداد

الخلاصة

يقدم هذا البحث تحليلاً تجريبياً ونظرياً لاستقصاء معامل انتقال الحرارة وانحدار الضغط خلال جريان ثنائي الطور في حالة غليان لمائع التثليج R134a في مقطع فحص لمبخر منظومة تجميد تحت ظروف تشغيل مختلفة. ظروف الاختبار التي اعتمدت في هذه الدراسة كانت، عند فيض حراري (13.7-36.6) كيلوواط\متر مربع، وفيض كتلي (52-105) كغم/متر مربع. ثانية ونسبة جفاف للبخار (0.2 - 1) ودرجة حرارة تشبع للمائع بين (-15 و -3.7) درجة مئوية. أجريت الاختبارات باستخدام جهاز أختبار لمنظومة تجميد سعتها 310W والتي صممت ونفذت خلال الدراسة الحالية. أظهرت النتائج التجريبية بان, تحسين

*Corresponding author
Peer review under the responsibility of University of Baghdad.
https://doi.org/10.31026/j.eng.2019.01.02

Article received: 25/1/2018
Article accepted: 13/3/2018

معامل انتقال الحرارة الموقعي للفيض الحراري الأعلى نسبيا$36.6kW/m^2$ كان بحدود 38%مقارنة بالفيض$13.7kW/m^2$ عند ظروف تشغيل ثابتة. تحسين معامل انتقال الحرارة عند زيادة قيمة الفيض الكتلي من 52 $kg/m^2.s$ الى 105 $kg/m^2.s$ خلال ظروف تشغيل مماثلة كان بنسبة 57%. وكان تحسين قيمة معامل انتقال الحرارة بنسبة 64% عند زيادة درجة حرارة التشبع من 8- الى3.7- عند ثبات قيم الفيض الكتلي والفيض الحراري. تأثير الفيض الكتلي على قيمة انحدار الضغط كان اعلى نسبيا بمقدار 27% من تأثير الفيض الحراري عند ظروف الاختبار المعتمدة. مقارنة النتائج التجريبية مع النظرية قد أظهرت توافق مقبول مع وجود نسبة تباين بينهما بحدود 21%.

الكلمات الرئيسية: انتقال الحرارة، انحدار الضغط، غليان الجريان، الفيض الحراري

1. INTRODUCTION

Boiling heat transfer is an effective mode of heat transfer that happens with a change in phase from liquid to vapor. Flow boiling heat transfer of environmental friendly refrigerant R134a is important in many fields, such as air conditioning, refrigeration, and thermal control systems. The flow boiling heat transfer process was investigated by many researchers in many thermal components and energy systems, as it gives important vital preferences in comparison with its single phase counterparts, much higher heat transfer coefficients, much smaller coolant flow rates, and better temperature uniformity. **Saitoh, et al., 2005** investigated experimentally flow boiling heat transfer of R-134a flowing through circular channels with three different internal diameters of 0.51, 1.12, and 3.1 mm. It is found that the heat transfer coefficient for the (0.51 mm) circular channel increased with increasing heat flux, but wasn't significantly affected by mass flux, while the heat transfer coefficient for the (3.1 mm) channel depended upon both heat flux and mass flux. **Park and Hrnjak, 2007** studied the boiling heat transfer coefficient and pressure drop in a horizontal smooth copper tube of 6.1 mm inner diameter for (CO_2, R410A, and R22) at mass flux from (100 to 400) kg/m^2.s, evaporation temperatures of -15 ºC and -30 ºC and heat flux from (5 to 15) kW /m^2 for vapor qualities ranging from (0.1 to 0.8). It is found that the flow boiling heat transfer of CO_2 is much higher than those for R410A and R22 especially at low vapor quality ranges for an identical heat flux, mass flux and evaporation temperature. The lower molecular weight and the higher pressure of CO_2 than those of the other refrigerants result in higher flows boiling heat transfer coefficients by enhancing the nucleate boiling heat transfer contribution. **Bertsch, et al., 2009** investigated the boiling heat transfer coefficient with R134a in multi-port rectangular micro-channels of hydraulic diameters of 1.09 and 0.54 mm. The measured parameter ranges are mass flux from 20 to 350 kg/m^2s , heat flux (0 – 220) kW/ m^2, saturation temperature (8 – 30) °C and vapor quality (0.2 to 0.9). It is found that the flow boiling heat transfer coefficient increases significantly with heat flux and weakly with mass flux and seems to be dominated by nucleate boiling. The pool boiling heat transfer for R-245fa is lower than R-134a as a result of its higher molecular mass and surface tension. **Del Col, et al., 2010** conducted an experimental investigation of flow boiling heat transfer for R134a, R125, R22 and R410A in 8 mm inner diameter horizontal tube with a mass flux of 200–600 kg/m^2.s, heat flux 9–53 kW/m^2, saturation temperature 25–45ºC, and vapor quality ranging from 0.07 to 0.87. It is found that the heat transfer coefficient increased with increasing heat flux and saturation temperature, but did not change significantly with mass flux. **Oh and Son, 2011** investigated heat transfer coefficients of R22 and R134a evaporating in horizontal copper tubes with inner diameters of 1.77 mm, 3.36 mm, and 5.35 mm in range of mass fluxes from 300 to 500 kg/m^2.s, heat fluxes of 10, 20, and 30 kW/m^2, temperatures of 0 and 5 ºC, and qualities from 0.05 to 0.97. It is found that the local heat transfer coefficient in the small diameter tubes (di < 6 mm) were observed to be strongly affected by inner diameter change and to differ from those in the large diameter tubes. The local evaporating heat transfer coefficients of 3.36 mm tube is about 15% higher than those of 5.35 mm tube, and the local heat transfer coefficients of 1.77 mm tube is about 20% higher than those of 3.36 mm tube. **Saisorn, et al., 2013** studied experimentally flow boiling heat transfer of R-134a in horizontal and vertical circular stainless steel mini-channels of

the internal diameter 1.75mm and 600 mm length to obtain flow visualization and heat transfer data. Two sets of the horizontal flow and vertical upward flow data are presented based on a heat flux range of 1–80 kW/m^2, mass flux range of 200–1000 kg/m^2.and a saturation pressure range of 7–13 bar. It is found that, flow visualization and heat transfer results show heat transfer coefficient depending on flow pattern. The results also indicate that flow regime transition and heat transfer coefficient tend to depend on flow direction under the certain experimental conditions. **Fang, et al., 2016,** presented the experimental results of the heat transfer coefficient of R-134a in three horizontal circular smooth copper tubes with different diameters of 1.002, 2.168 and 4.065 mm. Experimental data points are obtained for a mass flux range of 185–935 kg/m^2.s, a heat flux range of 18.0–35.5 kW/m^2, a saturation pressure range of 0.578–0.82 MPa, and a vapor quality range of 0.03–1.0. It is found that the heat transfer coefficient is higher for smaller tubes and for high saturation pressure while the effects of heat flux, mass flux, and vapor quality are different for different tubes. **Nguyen, et al., 2016** investigated the flow boiling heat transfer coefficient of R32 and R290 in horizontal stainless steel tubes with the inner diameter of 0.3 and 1.5 mm. The testing conditions were performed with the heat fluxes from 10 to 20 kW/m^2, the mass fluxes range from 200 to 500 kg/m^2.s, the saturation temperature of 10˚C and the vapor quality from 0.1 to dry-out. It is found that the heat transfer coefficient of the R32 and R290 increased with the increasing of heat flux and the frictional pressure gradient is higher with the highest mass flux and heat flux. A modified heat transfer coefficient correlation for alternative and natural refrigerants was proposed and predicted well the experimental data.

2. EXPERIMENTAL SETUP AND METHOD

2.1 Test Rig

The experimental setup is primarily consisting of reciprocating compressor with 125W capacity, water-cooled condenser, refrigerant flow meter, capillary tube, pre-heater, post-heater and test section which simulates the evaporator of the refrigeration system and two visualization sections installed at inlet and outlet of the test section with 150mm length glass tube of the same internal diameter of the test section as shown in **Fig.1** and **Fig.2**. Both of the pre-heater and post-heater sections consist of horizontal smooth copper tubes with 350mm length heated by electrically insulated tape resistance (400W) uniformly wrapped around the external tube surface to assure a uniform heat flux. The electrical power applied on pre-heater, test section, and post-heater are adjusted using three voltage controllers (variac transformer) with a rating from 0 V to 300 V, and 2 A to regulate the specified refrigerant vapor quality and saturation temperature at test section and at upstream and downstream of the test section. The high and low pressures of the refrigerant in the test rig system are measured using Bourdon pressure gauges with a range from 0 bar to 35 bar. Temperatures of the tube wall and refrigerant at different positions in the test rig are measured using K-type calibrated thermocouples with a range of -40 to 375 ˚C. Each junction of thermocouples was fixed on the tube and thermally insulated to reduce the effect of ambient conditions on the reading of thermocouples. Data loggers of model PCE-T 1200 with 12 channels are used to display the temperatures readings of the thermocouples. The locations of the thermocouples in the test rig are as shown in the **Fig.1**. Three thermostats with temperature control range (-40 ˚C to 99 ˚C), were used to control the temperatures of heating wires installed in the test section. The mass flux of the refrigerant is adjusted via bypass loop connected in parallel with test section line. The single-phase refrigerant enters the pre-heater as a subcooled liquid and heated to ensure the required vapor quality at test section entrance, and the heat flux imposed on the test section is regulated by voltage converter to maintain the specified test conditions.

2.2 Test Section

The test section in the experimental setup represents the evaporator section of a refrigeration system which is consisted of a horizontal smooth copper tube with inner diameter 5.8 mm, outer diameter 7.9 mm and 600 mm length. The test section tube was electrically heated to simulate the thermal load applied on the evaporator using a 400W heating resistance wire with length 2.5 m and uniformly wrapped around the outer wall of the test section tube to provide a uniform heat flux. The thermocouples are fixed with equal distances on the test section and the tube was wrapped with insulation material to minimize the heat loss caused by convection and radiation heat transfer with the ambient. The heat flux was regulated by varying the input electrical power using a variable power supply (variac). The inlet and outlet of the test section are connected with transparent tubes of 5.8 mm inner diameter and 150mm length for refrigerant flow visualization. The pressure drop along the test section tube was measured using two pressure transmitters installed at the inlet and outlet of the test section with a range from 0 bar to10 bar as shown in **Fig.3a.** In the test section, ten thermocouples are placed in five positions equally distributed along the test section tube. Two thermocouples are installed in each position at the top and bottom of the tube wall to measure the average value of the tube external surface temperature as depicted in **Fig3b**. To ensure a precise reading of the refrigerant temperature, the thermocouple bulb was inserted at the inlet and outlet of the test section tube as shown in **Fig.3c**.

2.3 Test Conditions

The experimental investigations of the refrigerant R134a flow boiling heat transfer coefficient and pressure drop in the evaporator test section are limited by operating conditions in the range of (13 – 36) kW/m^2 for heat flux, (52 -105) kg/m^2.s for mass flux, vapor quality (0.2 – 1) and saturation temperature (-15 to -3.7) °C as shown in the **table 1**.

3. DATA REDUCTION

An analysis is required to determine the flow boiling heat transfer coefficient and pressure drop from the experimental data as described below. The heat transfer coefficient and pressure drop calculation supposed the following considerations:
1-Heat transfer in the axial direction can be neglected.
2-Heat flux is uniform along the tube length in the test section.
3-Pressure drop in the test section is a linear function of tube length.

3.1 Heat Transfer Coefficient

The heat transfer rate supplied by heating resistance wire on the outside surface of the tube wall in the test section $\dot{Q}_{ev}$ is calculated by:

$$\dot{Q}_{ev} = V \cdot I \cdot \eta \quad (1)$$

Where: η is the heating coefficient that reflects the efficiency of the heat transfer process in the test section which can be determined by the following equation:

$$\eta = \frac{\dot{m} \cdot (h_o - h_i)}{P_e} \quad (2)$$

Where: P_e is the electrical power supplied to heating resistance wire wrapped around the tube in the test section which can be determined by the following equation:

$$P_e = V \cdot I \quad (3)$$

The heat flux q_{ev} supplied from inside tube wall surface in the test section to the refrigerant is calculated by **Fang**, **2016** and **Copetti, 2011.**

$$\dot{q}_{ev} = \frac{\dot{Q}_{ev}}{\pi \cdot di \cdot L_{ts}} \quad (4)$$

The heat fluxes applied at preheater and post heater can be determined using the same manner by Eq. (1), Eq. (2), Eq. (3) and Eq. (4).
The local heat transfer coefficient h_z was determined according to the Newton's cooling law:

$$h_z = \frac{\dot{q}_{ev}}{T_{wi} - T_{sat}} \quad (5)$$

Where: T_{sat} is the local refrigerant saturation temperature, and $T_{w.i}$ is the local internal tube wall temperature which was calculated assuming radial conduction through the tube wall as given by the following equation:

$$T_{wi} = T_{wo} - \dot{Q}_{ev} \cdot R_w \quad (6)$$

The local external tube wall temperature T_{wo} was assumed to be the average of measured temperatures around the tube cross section and calculated by the following equation:

$$T_{wo} = \frac{T_{wt} + T_{wb}}{2} \quad (7)$$

Where T_{wt} , T_{wb} are the external tube wall temperatures at the top and bottom of the test section tube respectively.
Thermal resistance R_w (˚C/W) of the test section tube is determined by **Incropera, 2007.**:

$$R_w = \frac{Ln\left(\frac{d_o}{d_i}\right)}{2\,\pi \cdot k_{cu} \cdot L_z} \quad (8)$$

L_z : is the local length along the test section tube.

The local saturation temperature at each position (z) along the test section tube $T_{sat.z}$ is calculated based on local saturation pressure $P_{sat.z}$ which could be expressed by:

$$P_{sat.z} = P_{i.ev} - \Delta p \cdot \frac{L_z}{L_{ts}} \quad (9)$$

Where: $P_{i.ev}\ is$ the refrigerant pressure at the inlet of the test section, Δp is the refrigerant pressure difference between inlet and outlet of the test section.

3.2 Refrigerant Vapor Quality

The vapor quality at the inlet of the test section x_{in} can be determined from energy balance in the preheater:

$$x_{in} = \frac{h_{i.ts} - h_{l.i}}{h_{fg.i}} \quad (10)$$

Where: $h_{l.i}$, $h_{fg.i}$ are the specific liquid and latent heat of vaporization enthalpies respectively at the test section.
$h_{i.ts}$: is the specific enthalpy of the refrigerant at the inlet of the test section and represents the enthalpy of the refrigerant at the outlet of preheater which can be determined by applying an energy balance on the pre-heater.

$$h_{i.ts} = h_{i.p} + \frac{\dot{Q}_{pre}}{\dot{m}} \quad (11)$$

Where $h_{i.p}$, is the refrigerant specific enthalpy at the inlet of the preheater.
The vapor quality of the refrigerant at each position x_z is calculated using a linear relation along test section length:

$$x_z = x_{in} + \Delta x \cdot L_z \quad (12)$$

Vapor quality difference Δx of the refrigerant between inlet and outlet of the test section can be expressed by:

$$\Delta x = \frac{x_o - x_i}{L_{ts}} \quad (13)$$

x_o : Vapor quality of the refrigerant at the outlet of the test section which is calculated by:

$$x_o = \frac{h_{o.ts} - h_{L.o}}{h_{lg.o}} \quad (14)$$

$h_{l.o}$: Specific enthalpy of the liquid refrigerant at the outlet of the test section.

$h_{Lg.o}$: Latent heat of vaporization of the refrigerant at the outlet of the test section.

$h_{o.ts}$: Specific enthalpy of the refrigerant at the outlet of the test section which is determined by applying an energy balance on the test section:

$$h_{o.ts} = h_{i.ts} + \frac{\dot{Q}_{ev}}{\dot{m}} \quad (15)$$

3.3 Frictional Pressure Drop

Total pressure gradient in the test section tube can be determined by **Padilla, 2011**:

$$-\frac{dp}{dz} = -\frac{\Delta p}{L_{ts}} \quad (16)$$

$$\Delta p = \Delta p_{fr} + \Delta p_m + \Delta p_{st} \quad (17)$$

Where:

Δp: Total pressure drop of the refrigerant flow in the test section tube (kPa) which is determined experimentally using the following equation:

$$\Delta p = P_{o.ev} - P_{i.ev} \quad (18)$$

$P_{i.ev}$, $P_{o.ev}$: Refrigerant pressures measured at the inlet and outlet of the test section tube respectively (kPa).

Δp_{fr}: Frictional pressure drop of the refrigerant flow due to shear at the tube surface and at the vapor-liquid interface in the test section (kPa).

Δp_m: Momentum pressure drop due to the acceleration of the two-phase refrigerant flow in the test section (kPa).

Δp_{st}: Pressure drop of the refrigerant flow due to the static pressure change in the test section tube (kPa).

Pressure drop Δp_{st} is neglected because the test section is a horizontal tube and thus no change in the static pressure along the tube, therefore from Eq.(17), Δp_{fr} is determined by:

$$\Delta p_{fr} = \Delta p - \Delta p_m \quad (19)$$

Where: Δp_m can be calculated using the homogeneous model by **Mancin, et al., 2016**:

$$\Delta p_m = G^2 . \left(\frac{1}{\rho_v} - \frac{1}{\rho_l}\right) . |\Delta x| \quad (20)$$

ρ_v, ρ_l: Vapor and liquid densities of the refrigerant in the test section respectively (kg/m^3).

$|\Delta x|$: The absolute value of the vapor quality change along the test section tube (for boiling and condensation cases).

3.4 Measurements Uncertainty

The uncertainty intervals of the calculated quantities are listed in **Table 2.**

4. RESULTS AND DISCUSSIONS

4.1 Characteristics of Refrigerant Flow Boiling

The variation of heat flux with wall and refrigerant temperature difference of flow boiling for several mass fluxes 52, 90 and 105 kg/m^{2}s is shown in **Fig.4** The mass flux 52 kg/m^2.s was the most affected by the variation in heat flux and temperature difference as a result of relatively low mass flow rate. Within this range (5 - 43)°C of temperature difference, the dominance of nucleate and forced convective contributions of flow boiling heat transfer is evident corresponding to a refrigerant boiling curve. The variation of the vapor quality during the refrigerant flow boiling process in the test section along the evaporator tube is depicted in **Fig.5** with fixed mass flux 90 kg/m^2.s and different heat fluxes. The changes in vapor quality with the normalized tube is evident in this figure as a result of the phase change process from liquid to vapor. A relatively higher vapor quality is noted at heat flux 36.6 kW/m^2 due to the variation in thermal load applied on the test section tube.

4.2 Effect of Heat Flux and Mass Velocity on Flow Boiling Heat Transfer Coefficient

Fig.6 illustrates the effect of heat flux in the range of 13.7 to 36.6 kW/m^2 on local heat transfer coefficient at fixed mass velocities 52 and 105 kg/m^{2}s. A significant variation of the heat transfer coefficient with vapor quality for all the values of heat flux can be seen in this figure due to the effect of nucleate and convective boiling contributions at this ranges of vapor quality and difference of wall-refrigerant temperatures corresponds to the refrigerant boiling curve. The heat

transfer coefficient was directly proportional with heat flux and relatively higher value of heat transfer coefficient was observed at heat flux 36.6 kW/m^2. The percentage increase in local heat transfer coefficient for relatively higher heat flux 36.6 kW/m^2 was about 38% compared to 13.7 kW/m^2 at constant operating conditions. The increase in heat flux at the fixed difference between tube surface and refrigerant temperatures enhance the value of heat transfer coefficient corresponds to Newton's law of convection heat transfer. A noticeable reduction in heat transfer coefficient was observed at higher vapor quality ($x > 0.8$) due to the dry out the effect of refrigerant boiling in the evaporator tube which occurs at relatively higher heat flux and low mass velocity. Similar behavior of heat transfer coefficient with vapor quality can be observed in this figure, but the range of values of local heat transfer coefficient at mass flux 105 kg/m^2 was higher than that for 52 kg/m^2.

4.3 Effect of Mass Flux on Flow Boiling Heat Transfer Coefficient

Fig.7 shows the variation of local heat transfer coefficient with vapor quality at fixed heat fluxes 13.7 kW/m^2 and 36.6 kW/m^2 for different mass fluxes 52, 90 and 105 kg/m^2.s. It is evident that the higher values of heat transfer coefficient are achieved by greater mass flux 105 kW/m^2 for both cases due to the contribution of forced convective evaporation. For constant test conditions, the enhancement in heat transfer coefficient was about 57% when the mass flux increased from 52 kg/m^2.s to 105 kg/m^2.s. The values of local heat transfer coefficient were relatively higher at 36.6 kW/m^2 compared to heat flux 13.7 kW/m^2 resulted from the rise of the thermal load applied on evaporator tube while the other test conditions maintained constant.

4.4 Effect of Saturation Temperature and Inlet Vapor Quality on Heat Transfer Coefficient

Fig.8 shows the effect of saturation temperature of the refrigerant R-134a on local heat transfer coefficient at constant heat flux 36.6 kW/m^2 and mass flux 105 kg/m^2. It can be seen for three different tested saturation temperature -3.7, -4 and -8˚C that, the increase of saturation temperature leads to a significant variation in the heat transfer coefficient. This behavior can be explained by the fact that, the increase of saturation temperature at constant test conditions will lead to enhancing heat transfer rate particularly at stratified flow-boiling region where the thickness of liquid film inside evaporator tube decreases and causes an increase in local boiling heat transfer coefficient. The enhancement in the heat transfer coefficient was about 64% when the saturation temperature increased from -8 to -3.7 ˚C at a fixed refrigerant mass velocity and heat flux. The effect of inlet vapor quality of the refrigerant on the local heat transfer coefficient in the evaporator tube at a fixed heat flux 36.6 kW/m^2 and mass flux 90 kg/m^2. s is illustrated in **Fig.9**. It can be observed for different values of the tested inlet vapor quality 0.18, 0.21, and 0.24 that, the local heat transfer coefficient tends to partially increase with inlet vapor quality through most values of local vapor quality in the evaporator tube due to the dominance of forced convective boiling at high vapor quality.

4.5 Effect of Mass Velocity and Heat Flux on Pressure Drop

Pressure drop during refrigerant flow boiling in the evaporator tube can result from three sources, the friction of fluid with tube surface, momentum change of the flow in the tube and static pressure change. The pressure drop resulted from static pressure is neglected because the tube is horizontal and no change in static head. The pressure drop resulted from momentum change has been determined and found no significant effect because the tube is of a symmetrical cross-section and no large change in flow acceleration, therefore only a frictional pressure drop is considered. **Fig.10** shows the pressure drop variation with vapor quality for two mass fluxes

(52 and 105 kg/m^2.s) and constant heat flux 36.6 kW/m^2. It can be noticed that, the pressure of the refrigerant for both mass fluxes increases with vapor quality along the evaporator tube, but the pressure drop for mass flux 105 kg/m^2.s was higher than that for 52 kg/m^2.s in the range of 7% due to the shear effect of the refrigerant flow on inner surface of the tube wall. **Fig.11** illustrates the pressure drop variation as a function of vapor quality for heat fluxes 22.8 and 36.6 kW/m^2 at constant mass flux 105 kg/m^2.s. The trend of the figure for both heat fluxes is approximately similar with a variation of vapor quality, but the pressure drop for heat flux 36.6 kW/m^2 was relatively higher than that for 22.8 kW/m^2 in the range of 3%.

4.6 Comparison Between Experimental and Predictive Models Results

4.6.1 Heat transfer coefficient

The experimental results of the present work are compared with the results of well-known predicted models in the literature, **Shah,1982**, **Gungor**, and **Winterton, 1986** and **Kandlikar, 1990.** These predicted results are calculated using EES software as depicted in the flowchart in **Fig.12**. based on similar operating conditions and plotted with experimental results for comparison. **Fig.13** shows the theoretical and experimental results of heat transfer coefficient as a function of vapor quality using three predicted models for mass flux 52 kg/m^{2}s at heat fluxes 18.3 kW/m^2 and 36.6 kW/m^2. It can be noticed from the figure that the theoretical models have well predicted the results within similar test conditions. The trend of the theoretical results is approximately similar to the experimental results with an average deviation in the range of (10%), (18%) and (36%) for Shah, Kandlikar and Gungor and Winterton models respectively for heat flux 18.3 kW/m^2 as shown in **Fig.13a**. This difference in results is due to the assumptions made to the theoretical models and measurement errors in the experimental work. While for heat flux 36.6 kW/m^2, the average deviation was in the range of (32%), (23%) and (32%) by Shah, Gungor and Winterton, and Kandlikar respectively as shown in **Fig.13b**. For constant heat flux, 36.6 kW/m^2 and two mass fluxes 90 and 105 kg/m^2.s, the comparison between predicted and experimental results of heat transfer coefficient as a function of vapor quality is shown in **Fig.14**. It can be observed in **Fig.14a** that, the values of predicted results were relatively higher than that for experimental results with a difference in the range of 21 %, 19 % and 36% by Shah, Gungor and Winterton and Kandlikar respectively. In **Fig.14b**, the average deviation between the predicted and experimental results was in the range of 10 %, 22 % and 15 % for Shah, Gungor and Winterton and Kandlikar respectively. It can be concluded that Shah model has shown the best prediction of heat transfer coefficient with experimental results compared to other models.

4.6.2 Pressure drop

The comparison between the experimental and theoretical results of the pressure drop predicted by the homogeneous flow model **Huang, 2011** along test section for several operating conditions is explained in the **Figs. 15**, **16** and **17**. The range of test conditions considered in this comparison was for mass fluxes 52 kg/m^2. s, 105 kg/m^2. s, and for heat fluxes 22.8 kW/m^2, 36.6 kW/m^2. The trend of the pressure gradient was almost similar for the experimental and theoretical results, and an increase along the axial position of the test section tube or with the rise of vapor quality can be observed due to the frictional effect of the tube wall. The average percentage difference between the experimental and theoretical results was in the range of (25%) of these figures.

The present work results are validated by comparing with other work results of **Fang, 2016**, which is found closer to the current work with some differences in the dimension of the test section and operating conditions. **Fig.18** shows the results comparison of the heat transfer coefficient as a function of vapor quality between the present work and **Fang, 2016**. It can be noticed that the trend of both results is approximately similar with some deviation resulted from the difference in operating conditions.

5. CONCLUSIONS

The experimental and theoretical results of the flow boiling heat transfer coefficient of the refrigerant R-134a in a smooth horizontal tube under different operating conditions for, heat flux, mass flux, vapor quality, and saturation temperature were presented. The behavior of the local heat transfer coefficient and pressure drop were investigated and the following conclusions can be derived:

1-The heat flux applied to the test section (evaporator channel) has a significant effect on refrigerant R-134a flow boiling heat transfer coefficient. The percentage increase in local heat transfer coefficient for relatively higher heat flux 36.6 kW/m^2 was about 38% compared to 13.7 kW/m^2 at constant operating conditions.
2- The local heat transfer coefficient was directly proportional to the refrigerant mass velocity. For constant test conditions, the enhancement in heat transfer coefficient was about 57% when the mass flux increased from 52 kg/m^2.s to 105 kg/m^2.s.
3- Within different tested values of the inlet vapor quality 0.18, 0.21, and 0.24, the local heat transfer coefficient was partially increased with inlet vapor quality along the length of the evaporator test section.
4- The effect of the saturation temperature on flow boiling local heat transfer coefficient was evident. The enhancement in the heat transfer coefficient was about 64% when the saturation temperature increased from -8 to -3.7 at a fixed refrigerant mass velocity and heat flux.
5- The pressure drop of the refrigerant flow in the evaporator tube was significantly affected by mass flux and heat flux, but the effect of mass flux on pressure drop was relatively higher by about 27% than that for heat flux at specified test conditions.
6-The comparison between the experimental and theoretical results has shown an acceptable agreement with average deviations in the range of 25 % in pressure drop, 21% and 15% in values of local heat transfer at prescribed heat flux and mass velocity respectively as predicted by Shah model compared to that for other models.

REFERENCES

- Bertsch, S. S., Groll, E. A., and Garimella, S. V., 2009, *Effects of Heat Flux, Mass Flux, Vapor Quality, and Saturation Temperature on Flow Boiling Heat Transfer In Microchannels*, International Journal of Multiphase Flow, Vol. 35, No.2, PP. 142-154.

- Chien, N. B., Vu, P. Q., Choi, K. I., and Oh, J. T., 2016, *An Experimental Investigation of Convective Boiling Heat Transfer Using Alternative and Natural Refrigerants Inside Horizontal Microchannels*, PP.1251-1261

- Copetti, J. B., Macagnan, M. H., Zinani, F., and Kunsler, N. L., 2011, *Flow Boiling Heat Transfer and Pressure Drop of R-134a In a Mini Tube*, Experimental Thermal and Fluid Science, Vol. 35, No.4, PP.636-644.

- Del Col, D., 2010, *Flow Boiling of Halogenated Refrigerants at High Saturation Temperature in A Horizontal Smooth Tube*, Experimental Thermal and Fluid Science, Vol. 34, No.2, PP. 234-245.
- Fang, X., Xu, Y., Li, G., Li, D., and Yuan, Y., 2016, *An Experimental Study of Flow Boiling Heat Transfer of R134a and Evaluation of Existing Correlations*, International Journal of Heat and Mass Transfer, Vol. 92, PP. 1143-115.
- Gungor, K. E., and Winterton, R. H. S., 1986, *A General Correlation For Flow Boiling in Tubes And Annuli*, International Journal of Heat and Mass Transfer, Vol.29, No.3, PP.351-358.
- Huang, J., 2011, *Performance Analysis of Plate Heat Exchangers Used As Refrigerant Evaporators*, Ph.D. Thesis, University of Witwatersrand.
- Incropera, F. P., Dewitt, D. P., Bergman, T. L., and Lavine, A. S.,2007, *Fundamentals of Heat and Mass Transfer*, Sixth Edition, John Wiley & Sons, U.S.A.
- Kandlikar, S. G., 1990, *A General Correlation For Saturated Two-Phase Flow Boiling Heat Transfer Inside Horizontal and Vertical Tubes*, ASME J. Heat Transfer, Vol.112, No.1, PP.219-228.
- Mancin, S., Zilio, C., Righetti, G., Doretti, L., and Longo, G. A., 2016, *R134a Flow Boiling inside a 4.3 mm ID Microfin Tube*, International Refrigeration and Air Conditioning Conference, PP. 1675-1675.
- Oh, H. K., and Son, C. H, 2011, *Evaporation Flow Pattern And Heat Transfer of R-22 And R-134a in Small Diameter Tubes*, Heat and Mass Transfer, Vol. 47, No.6, PP. 703-717.
- Padilla, M., Revellin, R., Haberschill, P., Bensafi, A., and Bonjour, J., 2011, *Flow Regimes And Two-Phase Pressure Gradient in Horizontal Straight Tubes: Experimental Results For HFO-1234yf, R-134a And R-410A*, Experimental Thermal and Fluid Science, Vol. 35, No.6, PP. 1113-1126.
- Park, C. Y., and Hrnjak, P. S., 2007, *CO 2 And R410A Flow Boiling Heat Transfer, Pressure Drop, And Flow Pattern At Low Temperatures in A Horizontal Smooth Tube*, International Journal of Refrigeration, Vol 30. No.1, PP. 166-178.
- Saisorn, S., Kaew-On, J., and Wongwises, S., 2013, *An Experimental Investigation of Flow Boiling Heat Transfer of R-134a In Horizontal And Vertical Mini Channels*, Experimental Thermal and Fluid Science, Vol.46, PP. 232-244.
- Saitoh, S., Daiguji, H., and Hihara, E., 2005, *Effect of Tube Diameter on Boiling Heat Transfer of R-134a in Horizontal Small-Diameter Tubes*, International Journal of Heat and Mass Transfer, Vol.48, No.23, PP.4973-4984.
- Shah, M. M., 1982, *Chart Correlation For Saturated Boiling Heat Transfer: Equations And Further Study*. ASHRAE Trans., United States, Vol.88 (CONF-820112).

NOMENCLATURE

d = diameter of the test section tube, m.
G = mass flux (mass velocity), $G= \dot{m} /(\pi \cdot d^2/4)$, $kg/m^2.s$.
h = specific enthalpy, kJ/kg.

h_{fg} = latent heat of vaporization, kJ/kg.
h_z = local heat transfer coefficient, W/m^2.C.
I = current, A
k_{cu} = thermal conductivity, W/m.˚C.
L = length of the test section tube, m.
Lz = length of tube subsection, m.
$\dot{m}$ = refrigerant mass flow rate, kg/s.
P = pressure, Pa.
$\dot{Q}$ = heat transfer rate, W.
q_{ev} = heat flux, W/m^2.
R_w = thermal resistance, ˚C/W
T = temperature, ˚C.
V = voltage, V
x = vapor quality, dimensionless.

Subscripts

av = average
b = bottom
cu = copper
ev = evaporation
fr = frictional
i = inlet
l = liquid
m = momentum
o = outlet
pre = preheater
sat = saturation
t = top
ts = test Section
v = vapor
w = wall

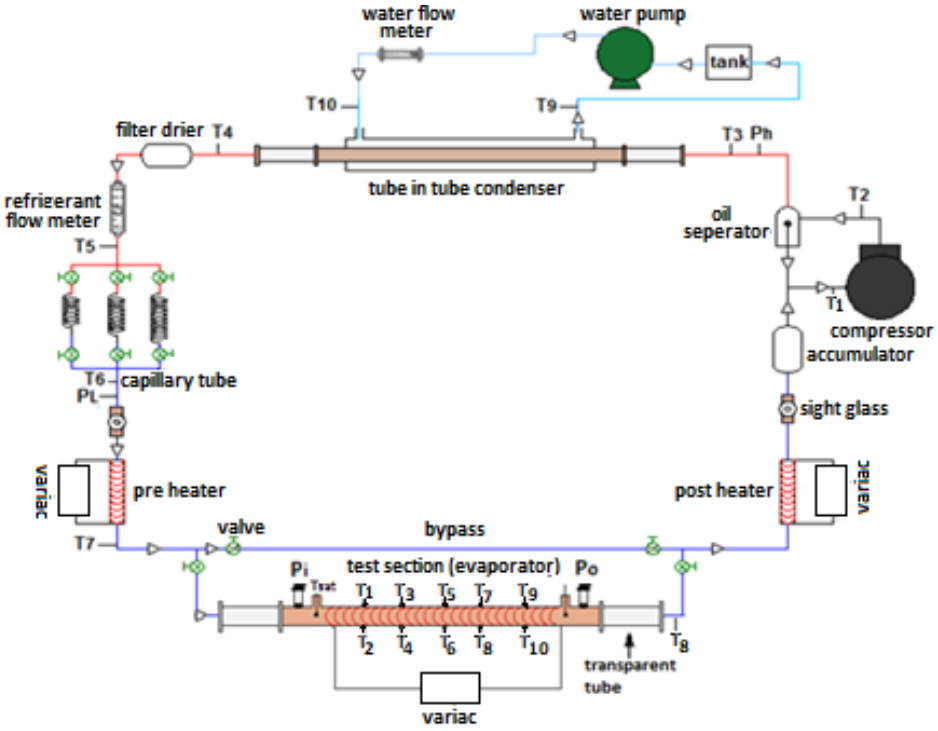

Figure 1. Schematic diagram of the refrigeration system.

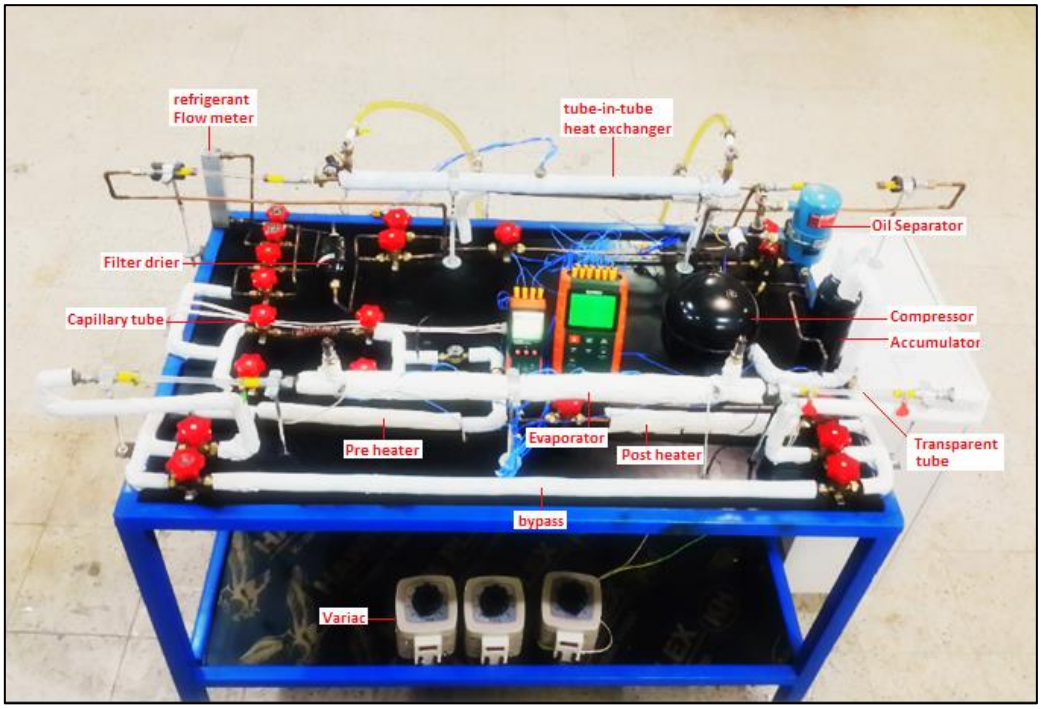

Figure 2. Experimental setup.

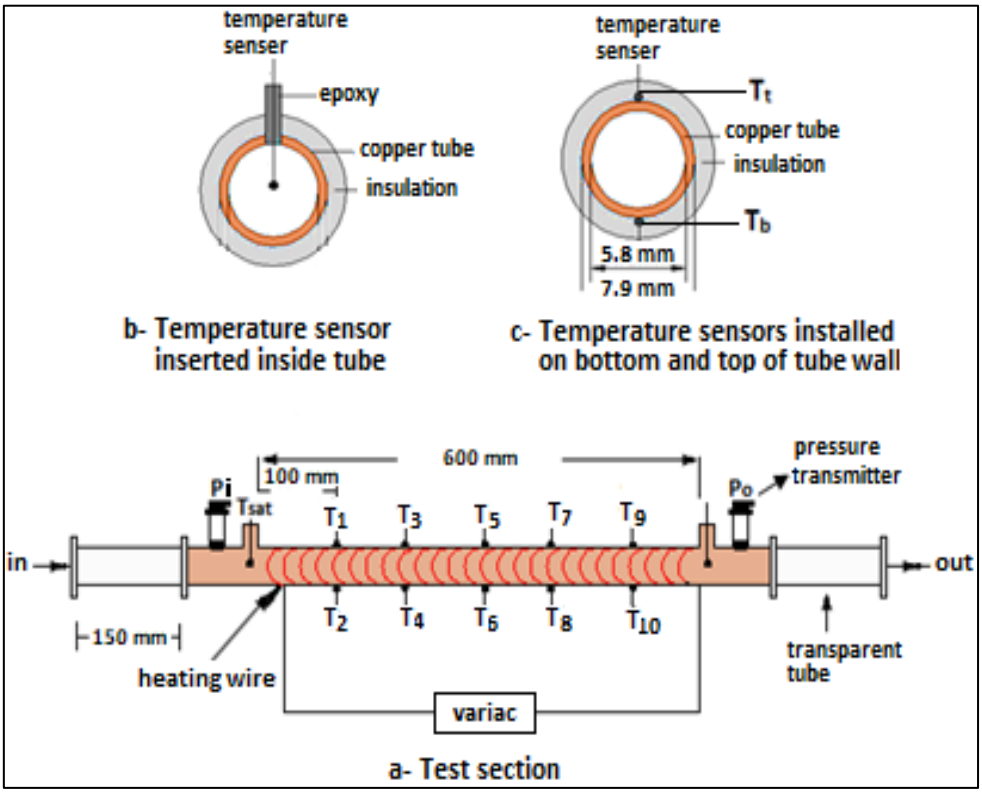

Figure 3. Schematic of the test section.

Table 1. Operating conditions considered in the present study.

No	Mass Flux ($kg/m^2.s$)	Heat Flux (kW/m^2)				
1	52	13.7	18.3	22.8	27.4	36.6
2	90	13.7	18.3	22.8	27.4	36.6
3	105	13.7	18.3	22.8	27.4	36.6
	Range of vapor quality: X = 0.2 - 1					
	Range of evaporating temperature: -15 to -3.7					

Table 2. Uncertainties of the calculated quantities.

Quantity	Uncertainty
Local heat transfer coefficient h_z. $(W/m^2.^{\circ}C)$	$\pm$ 18
Local saturation pressure $P_{sat.z}$. (bar)	$\pm$ 0.22
Local vapor quality x_z.	$\pm$ 0.04
Heating power $\dot{Q}_{ev}$. (W)	$\pm$ 2.55

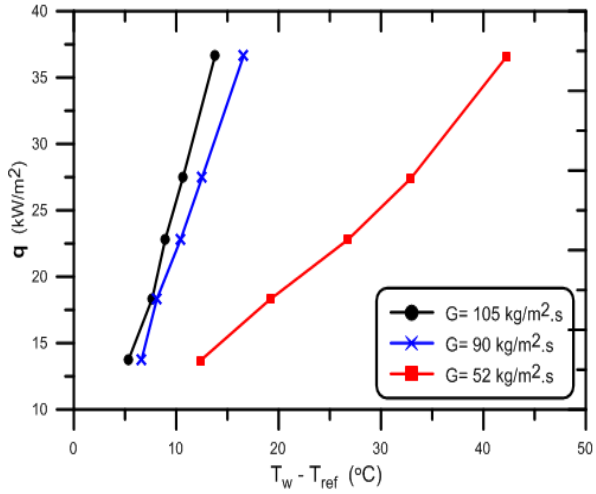

Figure 4. Variation of heat flux with wall and test refrigerant temperature difference for several mass fluxes.

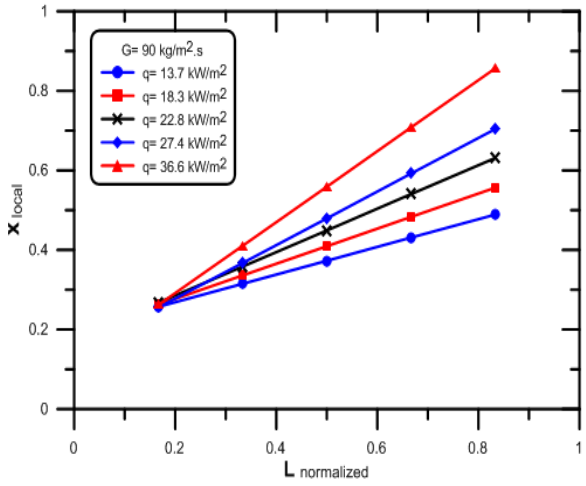

Figure 5. Vapor quality as a function of section length for different heat fluxes.

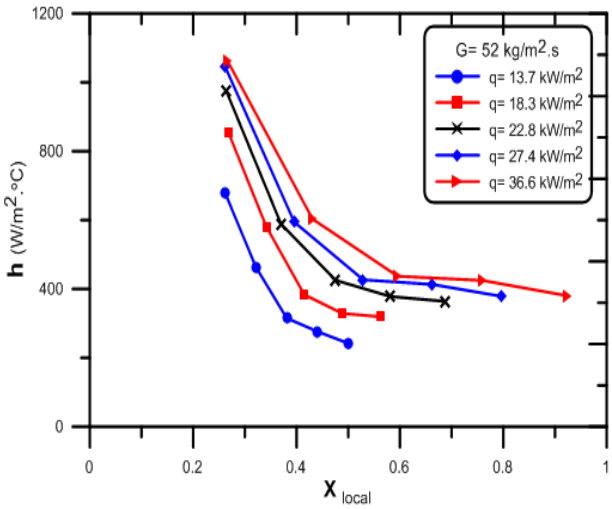

a) G = 52 (kg/m^2.s)

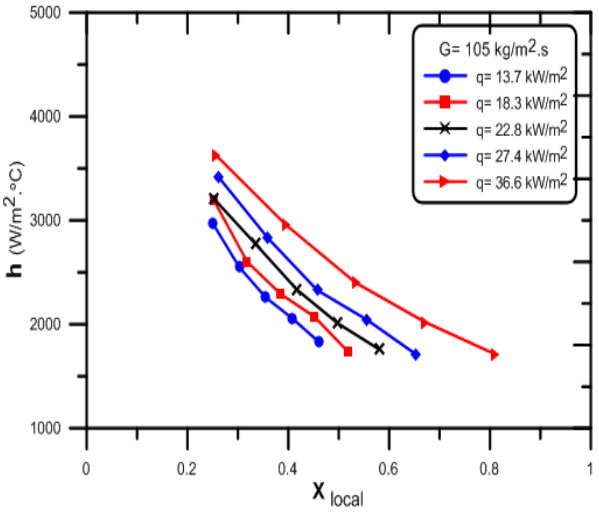

b) G = 105 (kg/m^2.s)

Figure 6. Effect of heat flux on the local heat transfer coefficient for mass fluxes **(a)** 52 (kg/m^2.s) and **(b)** 105 (kg/m^2.s).

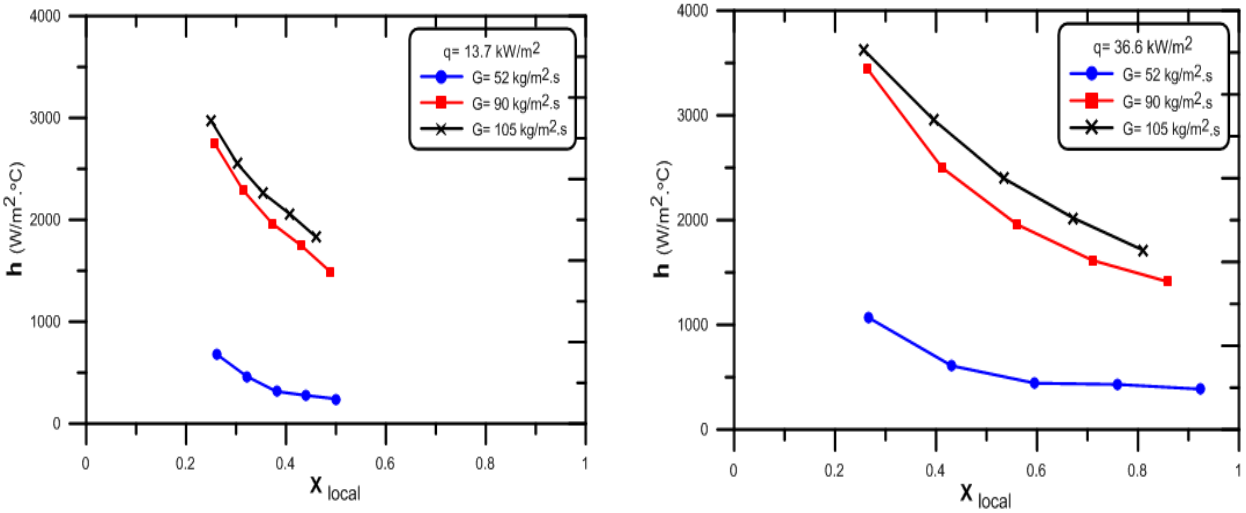

a) q = 13.7 (kW/m^2) **b)** q = 36.6 (kW/m^2)

Figure 7. Effect of mass flux on local heat transfer coefficient for heat fluxes **(a)** 13.7 (kW/m^2) and **(b)** 36.6 (kW/m^2).

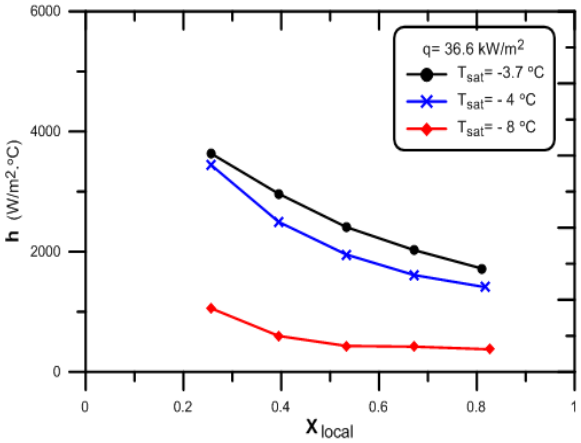

Figure 8. Effect of saturation temperature on
local heat transfer coefficient for q=36.6 kW/m^2.

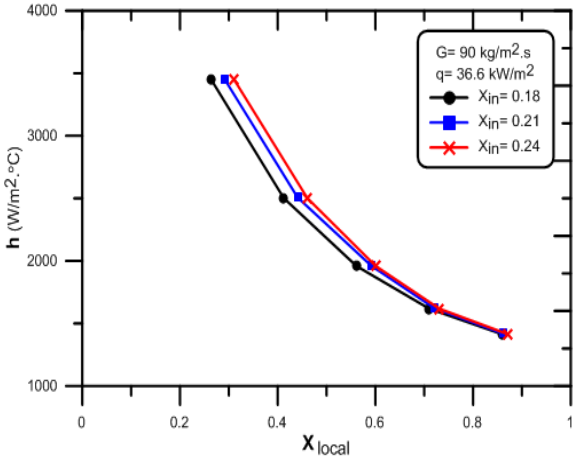

Figure 9. Effect of inlet vapor quality on local heat transfer coefficient for q=36.6 kW/m^2 and G = 90 kg/m^2.s.

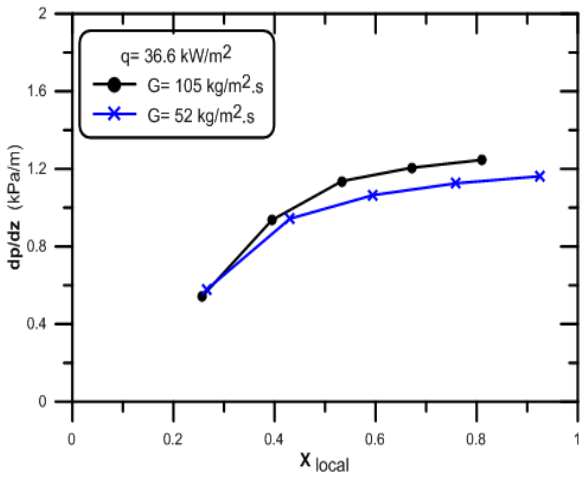

Figure 10. Effect of mass velocity on pressure drop for heat flux 36.6 kW/m^2.

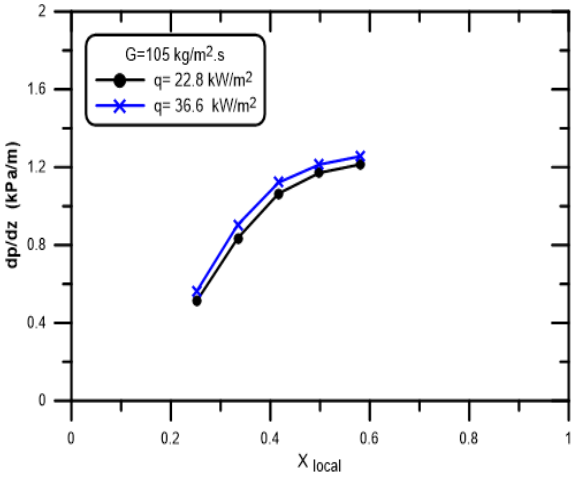

Figure 11. Effect of heat flux on pressure drop for mass velocity 105kg/m^2.s.

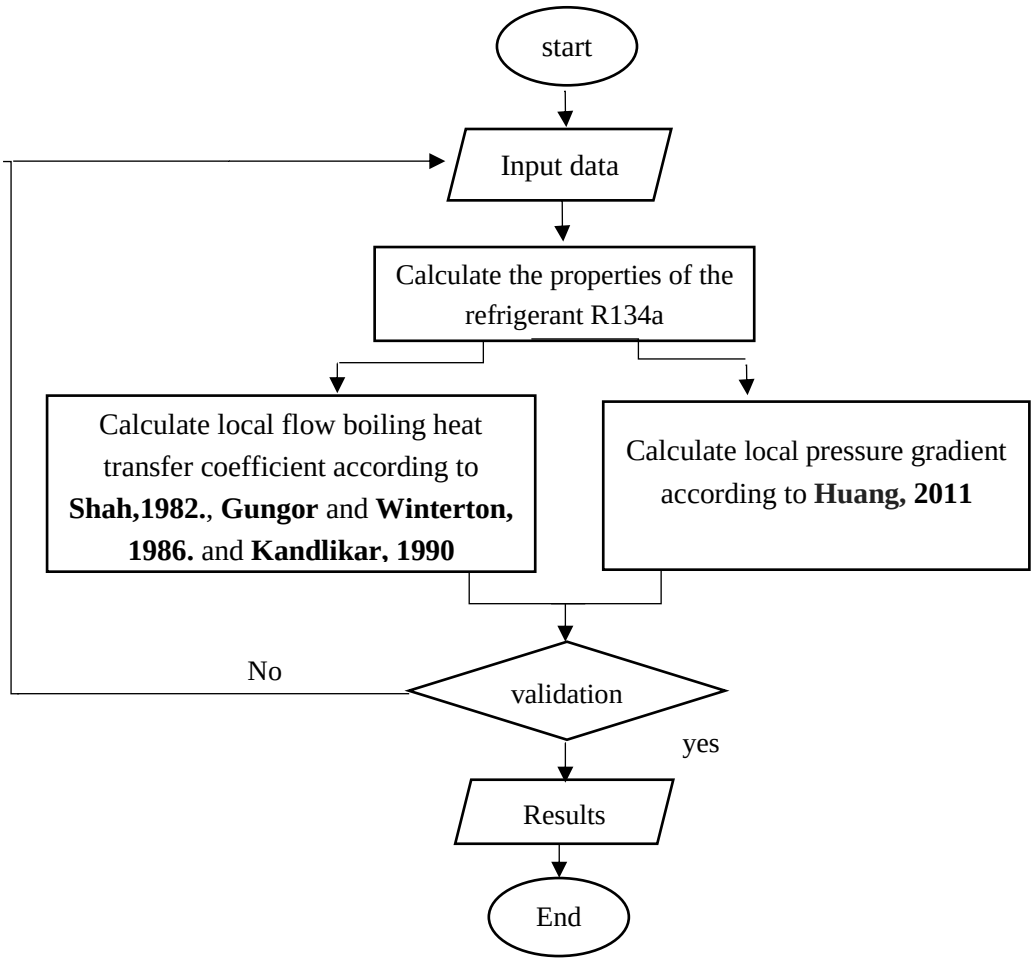

Figure 12. Flow chart of the predicted results.

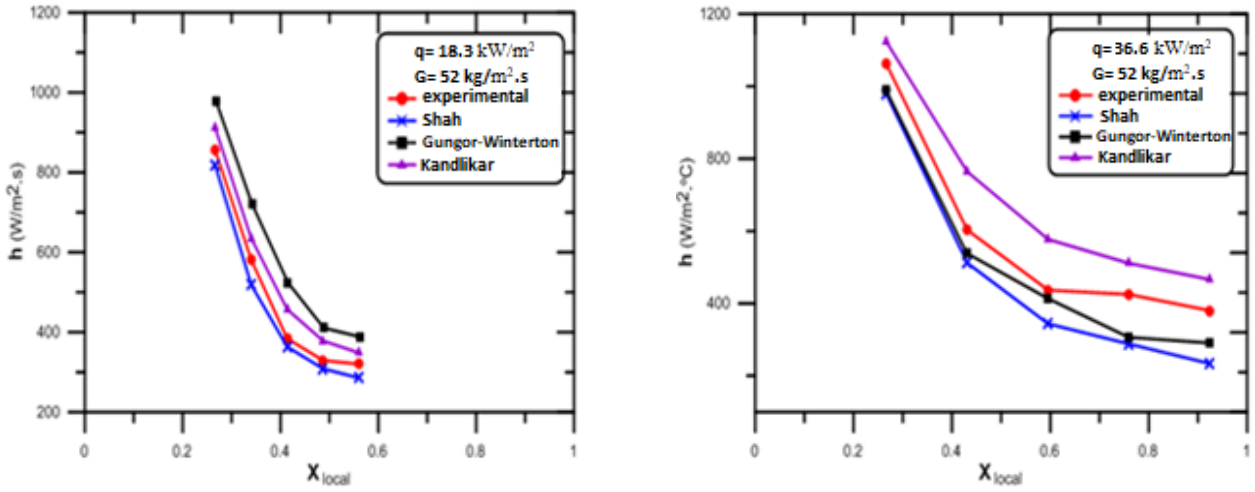

a) q =18.3 kW/m^2 **b) q** =36.6 kW/m^2

Figure 13. Predicted and experimental heat transfer coefficient as a function of vapor quality for mass velocity 52 kg/m^2.s and heat flux (**a**) 18.3 kW/m^2 , (**b**) 36.6 kW/m^2 .

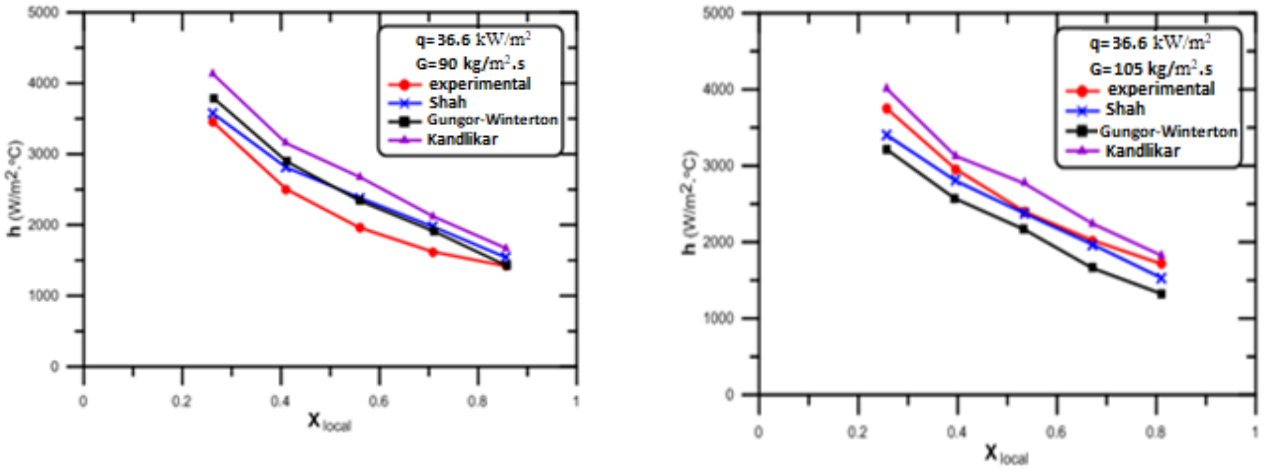

a) G = 90 (kg/m^2.s) **b) G** =105 (kg/m^2.s)

Figure 14. Predicted and experimental heat transfer coefficient as a function of vapor quality for heat flux 36.6 (kW/m^2) and mass velocity **(a)** 90, **(b)** 105 (kg/m^2.s).

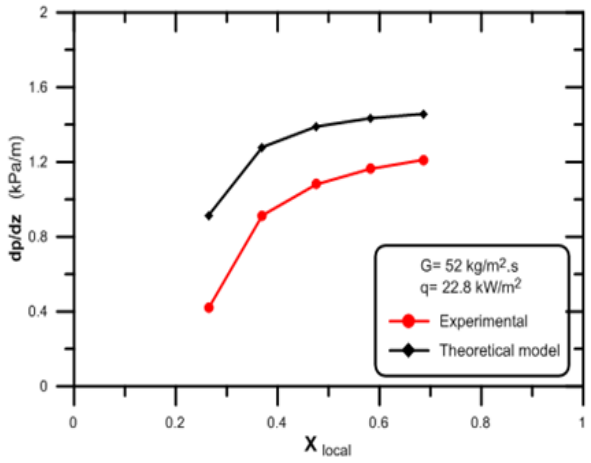

Figure 15. Experimental and theoretical pressure drop as a function of vapor quality for G=52 kg/m^2.s and q=22.8 kW/m^2.

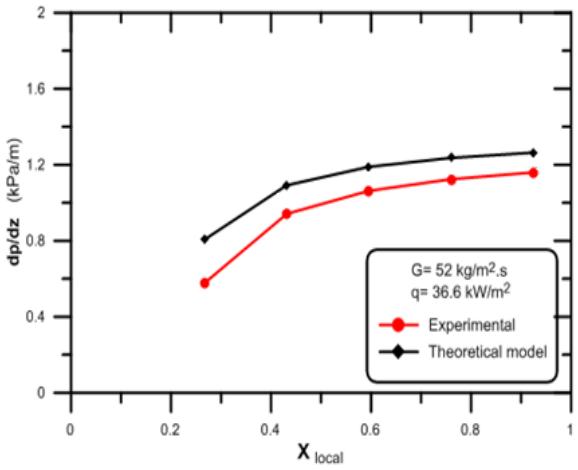

Figure 16. Experimental and theoretical pressure drop as a function of vapor quality for G=52 kg/m^2.s and q=36.6 kW/m^2.

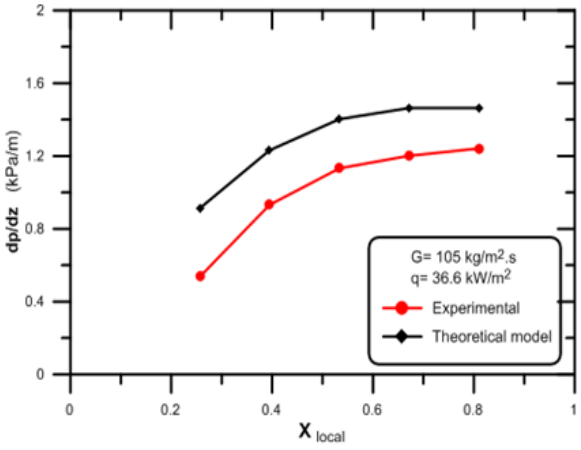

Figure 17. Experimental and theoretical pressure drop as a function of vapor quality for G= 105 kg/m^2.s and q= 36.6 kW/m^2.

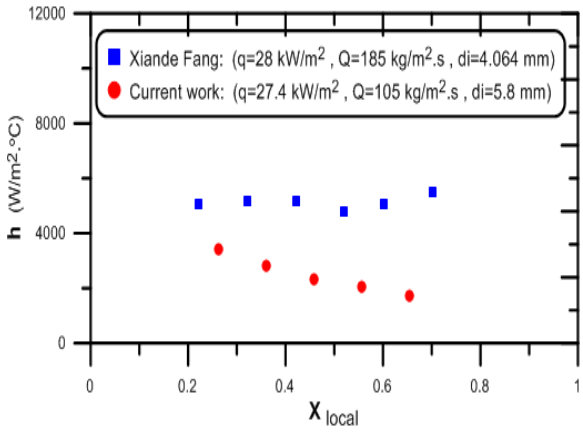

Figure 18. Comparison of the present work and **Fang, 2016**, results.